Orbital-dependent metamagnetic response in $Sr_4Ru_3O_{10}$

Y. J. Jo,[1] L. Balicas,[1] N. Kikugawa,[2,*] E. S. Choi,[1] K. Storr,[3] M. Zhou,[4] and Z. Q. Mao[4]
[1]*National High Magnetic Field Laboratory, Florida State University, Tallahassee, Florida 32306, USA*
[2]*School of Physics and Astronomy, University of St. Andrews, St. Andrews, Fife KY16 9SS, United Kingdom*
[3]*Department of Physics, Prairie View A&M University, Prairie View, Texas 77446-0519, USA*
[4]*Department of Physics, Tulane University, New Orleans, Louisiana 70118, USA*
(Received 28 January 2007; published 13 March 2007)

We show that the metamagnetic transition in $Sr_4Ru_3O_{10}$ bifurcates into two transitions as the field is rotated away from the conducting planes. This two-step process comprises partial or total alignment of moments in ferromagnetic bands followed by an itinerant metamagnetic transition whose critical field increases with rotation. Evidence for itinerant metamagnetism is provided by the Shubnikov–de Haas effect, which shows a nontrivial evolution of the geometry of the Fermi surface and an enhancement of the quasiparticles effective mass across the transition. We conclude that the metamagnetic response of $Sr_4Ru_3O_{10}$ is orbital dependent and involves both ferromagnetic and metamagnetic bands.

DOI: 10.1103/PhysRevB.75.094413 PACS number(s): 75.30.−m, 71.18.+y, 72.15.Gd

I. INTRODUCTION

Metamagnetism is usually understood as a rapid increase of the magnetization of a given system in a narrow range of magnetic fields. In a spin-localized picture, it would correspond to the field-induced suppression of, for instance, antiferromagnetic order via a spin-flop or the subsequent spin-flip transition.[1] In itinerant systems, metamagnetism is explained either in terms of the field-induced spin polarization of the Fermi surface and concomitant field-tuned proximity of the Fermi level to a van Hove singularity[2] or in terms of the suppression of antiferromagnetic correlations.[1] So far, both itinerant metamagnetic scenarios have been discussed within a single band picture.[1,2]

The ruthenates, $Sr_3Ru_2O_7$ in particular, were reported to display complex metamagnetic behavior, including the possibility of quantum criticality by tuning to zero temperature the end point of a first-order metamagnetic transition.[3] At low temperatures and in high-purity samples, this first-order line bifurcates into two first-order transitions that define the boundary of a new phase[4] emerging at the quantum-critical end point, which is claimed to result from the coupling of lattice fluctuations to a Fermi-surface instability.[5] Complex and highly anisotropic metamagnetic behavior has also been recently reported in the trilayered $Sr_4Ru_3O_{10}$ compound,[6] which is a structurally distorted ferromagnet: the RuO_6 octahedra in the outer two layers of each triple layer are rotated by an average of 5.6° around the c axis, while the octahedra of the inner layers are rotated in the opposite sense by an average of 11.0°.[7] It displays a Curie temperature $T_c \sim 100$ K (see the upper panel of Fig. 1, which shows the temperature dependence of both the heat capacity C normalized with respect to the temperature T as well as the low-field magnetization m) and a saturated moment $S \gtrsim 1\mu_B$ per Ru^{4+} ion, which Raman spectroscopy suggests to be *localized* in the Ru site[8] and directed essentially along the c axis.[6,7] The ferromagnetic (FM) transition is followed by an additional broad peak in the magnetic susceptibility at $T_M \simeq 50$ K in flux-grown samples[6,7] ($T_M \simeq 70$ K in floating zone-grown crystals), which is claimed to result from the "locking" of the moments into a canted antiferromagnetic configuration.[8] Nevertheless, neutron-scattering experiments indeed find the moments lying in the *ab* plane but coupled ferromagnetically.[9] Furthermore, the behavior of the magnetic susceptibility m/H, shown in Fig. 1, displaying a ferromagnetic transition followed by a broad maximum as the temperature is lowered, is consistent with the reentrance of the paramagnetic state at lower temperatures, a conventional behavior of itinerant metamagnetic systems close to a van Hove singularity.[1,2] Here we show that $Sr_4Ru_3O_{10}$ displays clear evidence for metamagnetic behavior involving simultaneously, several of the bands associated with the t_{2g} orbitals.

II. RESULTS AND DISCUSSION

Figure 2(a) displays the magnetization m of a $Sr_4Ru_3O_{10}$ single crystal measured with a commercial SQUID magnetometer as a function of the field H at $T=5$ K and for several values of the angle θ between H and the c axis. When H is applied along an in-plane direction ($\theta=90°$), it exhibits a sharp and hysteretic metamagnetic transition at a critical field $H_{MM} \sim 2.5$ T.[6,7] In high-quality single crystals the ob-

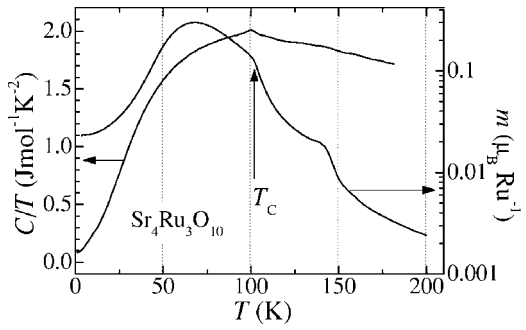

FIG. 1. Heat capacity C normalized with respect to temperature T and magnetization m (for a field of 500 G applied along an in-plane direction) for a $Sr_4Ru_3O_{10}$ single crystal and as a function of temperature T. Only one single anomaly, the Curie temperature, is observed in *both* traces at $T_c \sim 100$ K.

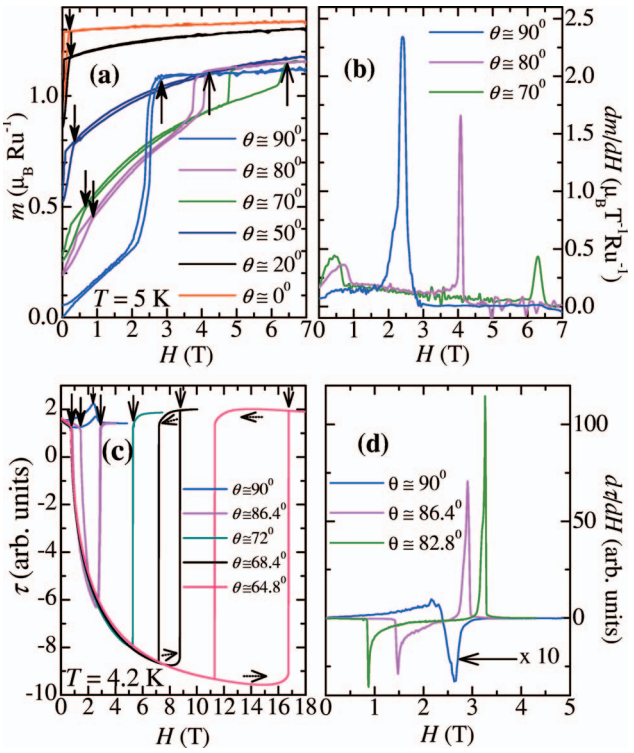

FIG. 2. (Color) (a) Magnetization m as a function of field H for several angles θ between H and the interplane c axis. Arrows indicate the metamagnetic transitions. (b) The derivative of m with respect to the field $\partial m/\partial H$ and as a function of field H displaying peaks at the metamagnetic transitions. (c) Magnetic torque τ as a function of H at 4.2 K. The vertical arrows indicate the metamagnetic transitions. The dotted arrows indicate increasing or decreasing field sweeps. (d) The derivative of the torque τ with respect to the field $\partial\tau/\partial H$ and as a function of field H.

served hysteresis exhibits ultrasharp steps in the resistivity resulting from domain formation.[10] But as θ decreases, as indicated by the vertical arrows, the transition clearly occurs via an anisotropic two-step process. A first step in m is observed at $\sim$1 T and moves to lower fields as θ decreases leading at high angles and above a field of just 0.2 T, to a saturation value $m \simeq 1.3\mu_B$ per Ru. Notice that according to Hund's rule, the placement of the four Ru^{+4} carriers on the three $4d$ t_{2g} orbitals leads to an effective moment $S=1$ or $2\mu_B$ per Ru. If the lattice distortions in $Sr_4Ru_3O_{10}$ do not lift the degeneracy among the three t_{2g} orbitals, one would expect each orbital to contribute 2/3 of a μ_B per Ru to the total moment. Thus a saturation value of $2\times 2/3 \simeq 1.3\mu_B$ per Ru suggests the polarization of the moments in *two* of the t_{2g} orbital networks, while a second step is observed in the magnetization when $\theta < 90°$ and moves to much higher fields as θ decreases producing considerable hysteresis. This behavior is confirmed by measurements of the magnetic torque $\vec{\tau} = n\vec{m} \times \vec{H}$ (where n is the total number of Ru atoms) measured by using a thin-film CuBe cantilever (5/1000 of an inch in thickness) at $T=4.2$ K shown in Fig. 2(b). Notice how sharp and hysteretic this second metamagnetic transition is. Its sharpness is a very strong indication of the high quality of our samples. Remarkably, at low angles this second metamagnetic transition occurs under a sizable component of H applied along the interplane direction, or with the moments basically aligned along the c axis by the first transition.

In order to understand this complex metamagnetic behavior, particularly the high field metamagnetic transition, we performed electrical-transport measurements at very high magnetic fields and low temperatures in two batches of single crystals, one having a residual resistivity $\rho_0 \simeq 6$ $\mu\Omega$ cm, where we performed interplane transport measurements, and a second one displaying a ρ_0 between 1.5 and 2 $\mu\Omega$ cm used mainly for in-plane transport studies. Our goal is twofold: (i) to measure the evolution of the geometry of the Fermi surface and of the quasiparticles effective mass across the high-field metamagnetic transition via the Shubnikov–de Haas effect, to explore the possibility of itinerant metamagnetism and (ii) to determine the geometry of the Fermi surface in order to stimulate band-structure calculations, which could clarify the possible existence of localized bands.

Our crystals were grown by a floating-zone (FZ) technique.[11] Crystals selected for the measurements were characterized by x-ray diffraction, heat capacity, and magnetization measurements and were found to be pure $Sr_4Ru_3O_{10}$. For instance, in Fig. 1, only one weak anomaly is seen in C/T at $T_c \simeq 100$ K indicating the onset of ferromagnetism. No clear anomaly is seen that one could associate with the proposed spin-canting transition[8] or with the existence of inclusions of other phases. The absence of inclusions, as seen for example, in self-flux-grown samples,[12] is confirmed by measurements of the magnetization m as a function of T for a field of $H=500$ G applied along an in-plane direction, also shown in Fig. 1. One sees only a couple of anomalies, one at T_c and a second one at 140 K, which does not leave any clear signature in C/T. Inclusions of $SrRuO_3$ would produce an anomaly at $T_c=160$ K and would lead to a rapid increase in m when low fields are applied along the ab plane, contrary to what is seen, respectively, in Figs. 1 and 2(a). Electrical-transport measurements were performed by using conventional four-probe techniques in conjunction with a single-axis rotator inserted in a ^{3}He cryostat. High magnetic fields up to 45 T were provided by the National High Magnetic Field Laboratory.

Figure 3(a) shows the interplane resistivity ρ_{zz} for two $Sr_4Ru_3O_{10}$ single crystals (typical dimensions $0.5\times 0.5 \times 0.3$ mm^3) at $T \simeq 0.6$ K as a function of H and for several angles θ between H and the interplane c axis. Notice both the oscillations in ρ_{zz} or the Shubnikov–de Haas (SdH) effect, and the marked negative magnetoresistivity *emerging from the second metamagnetic transition* seen at higher fields. For $\theta \simeq (12\pm 2)°$, for example, the metamagnetic transition field is $\sim$34 T (blue trace), and is displaced to fields beyond 45 T as the field is aligned along the c axis. Figure 3(b) displays the oscillatory component or the SdH signal [defined as $(\sigma - \sigma_b)/\sigma_b$, where $\sigma = 1/\rho$ and σ_b is the inverse of the background resistivity] of the trace shown in (a) [$\theta \simeq (12\pm 2)°$] as a function of the inverse field H^{-1}. Both the amplitude and the frequency of the oscillatory component changes drastically at $H_{MM} \sim 34$ T as quantified by the fast-Fourier transform of the SdH signal taken in two limited field ranges, i.e.,

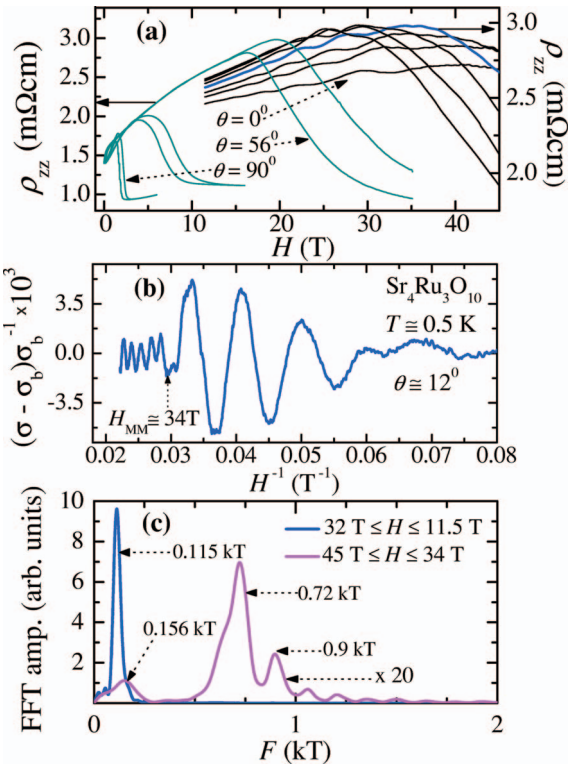

FIG. 3. (Color) (a) The interplane resistivity ρ_{zz} for two $Sr_4Ru_3O_{10}$ single crystals as a function of magnetic field H at $T \simeq 0.5$ K and for several angles θ between H and the interplane c axis. Notice both the presence of Shubnikov–de Haas oscillations and the rapid decrease in ρ_{zz} when the metamagnetic transition is crossed at higher angles. (b) The SdH signal $(\sigma - \sigma_b)\sigma_b^{-1}$, where $\sigma_b = 1/\rho_b$ is the background conductivity as a function H^{-1} for the blue trace at $\theta = 12 \pm 2°$ in (a). (c) The fast-Fourier transform (FFT) of the SdH signal in (b) for two ranges in field, i.e., above and below the metamagnetic transition.

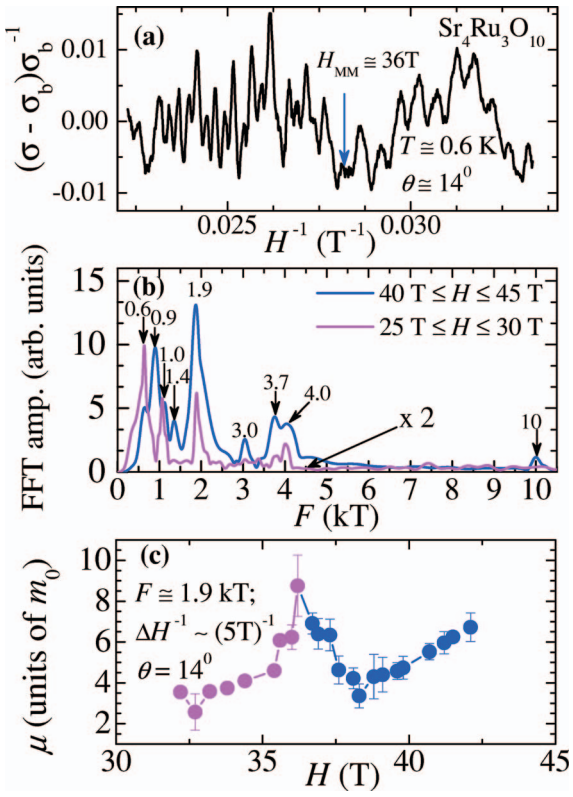

FIG. 5. (Color) (a) Oscillatory component of the in-plane resistivity ρ for a $Sr_4Ru_3O_{10}$ single crystal as a function of H at $T \simeq 0.6$ K and for $\theta = (14 \pm 2)°$ between H and the interplane c axis. (b) The FFT spectrum of the SdH signal shown for two limited-field ranges, from 25 to 30 T (in magenta) and from 40 to 45 T (in blue). Arrows indicate the frequency of the main peaks in kT. (c) The magnetic-field dependence of the effective mass associated with the FFT peak at $F = 1.9$ kT. The temperature dependence of the FFT spectra was taken within a window in $\Delta(H)^{-1} \simeq (5\text{ T})^{-1}$.

from 11.5 to 32 T (or below H_{MM}) in blue and from 34 to 45 T (or above H_{MM}) in magenta, both shown in Fig. 3(c). The peak seen at $F = 115$ T (Ref. 6) is completely suppressed by the transition implying the reconstruction of the Fermi surface.

A more thorough investigation of the effect of the transition on the Fermi surface is given by measurements of the in-plane magnetoresistivity $\rho(H)$ in the highest-quality single crystals of $Sr_4Ru_3O_{10}$ (dimensions $0.6 \times 0.6 \times 0.04$ mm^3) currently available. As an example of typical raw data, we show in Fig. 4 the in-plane resistivity as a function of the external field in a limited range, i.e., between 30 and 45 T at $T = 0.6$ K, and for an angle $\theta \simeq 14°$. The SdH oscillations are

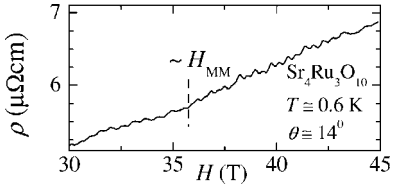

FIG. 4. In-plane resistivity $\rho(H)$ as a function of field H in a limited-field range for $T = 0.6$ K and $\theta = 14°$.

clearly visible although the metamagnetic transition is barely perceptible. Notice how $Sr_4Ru_3O_{10}$ is extremely anisotropic ($\rho_{zz}/\rho \sim 1000$); consequently, one should expect to observe nearly two-dimensional Fermi-surface sheets. Figure 5(a) shows the SdH signal obtained from the trace of $\rho(H)$ in Fig. 4. According to Fig. 2(a), at this angle under a field of 7 T the net moment is nearly saturated to a value of $\sim 1.3\mu_B$. While from our previous angular study in Fig. 3(a), at this angle one expects the metamagnetic transition to happen in the neighborhood of 35 T. One can clearly see that the oscillatory pattern changes at $\simeq 36$ T. In Fig. 5(b) we display the FFT spectrum of the SdH signal for two ranges of magnetic field, i.e., from 25 to 30 T or clearly below the metamagnetic transition (in magenta), and from 40 to 45 T where the geometry of the Fermi surface is closer to being stable (in blue). Larger frequencies such as the one at ~ 2 kT and those around 4 kT, remain unaffected by the transition. However, the entire spectral weight below 2 kT is shifted towards higher frequencies. This situation is somewhat similar to that reported in the bilayered compound $Sr_3Ru_2O_7$ where the FFT spectrum reveals additional structure and small shifts in the frequency of the main peaks across its metamagnetic transition, which are claimed to result from the spin splitting of the

Fermi surface.[13] In Fig. 5(c) we plot the effective mass μ in units of free-electron mass m_0, associated with the peak observed at $F=1.9$ kT and as a function of H. Here we measured ρ at different temperatures and extracted the corresponding FFT spectrum within a narrow window in $H^{-1} \sim (5\ \mathrm{T})^{-1}$. The evolution of the amplitude of a given peak in frequency as a function of temperature was fitted to the usual Lifshitz-Kosevich expression $x/\sinh x$ to extract μ. Notice how the value of μ spikes at ~36 T, a behavior similar to that of $Sr_3Ru_2O_7$ and which is claimed to result from the fluctuations emerging from a metamagnetic quantum-critical end point.[13] A metamagnetic quantum-critical end point in the context of itinerant metamagnetism has also been predicted for $Sr_4Ru_3O_{10}$ (Ref. 2) but more work is needed to clarify its existence. In any case, the enhancement of effective mass is also consistent with the scenario of a Zeeman-split Fermi surface that crosses a nearby Van Hove singularity as the field increases, i.e., conventional itinerant metamagnetic scenario.

In $Sr_4Ru_3O_{10}$ the amplitude of the oscillations is quickly damped as θ increases. However, we were able to fit (not shown here) the angular dependence of the main peaks corresponding, respectively, to 1.9, 3.95, and 9.96 kT, and which are associated with the largest cross-sectional areas of the Fermi surface, to the expression $F=F_0/\cos\theta$, indicating their two-dimensional character. Instead, lower frequencies such as the ~1 kT display a linear dependence. Although one could naively expect $Sr_4Ru_3O_{10}$ to display a nearly three-dimensional Fermi surface due to its structural proximity to the infinite-layered compound $SrRuO_3$, the two-dimensional character of its main Fermi surface sheets agrees well with its highly anisotropic electrical-transport properties. Finally, the effective masses associated with these orbits averaged over our entire field range are 4.4 ± 0.5, 5.6 ± 0.3, 6 ± 1, and 21 ± 6 for the 1.02, 1.9, 3.95, and 9.96 kT frequencies, respectively.

III. CONCLUSIONS

In summary, we have shown that the metamagnetic behavior observed in $Sr_4Ru_3O_{10}$ *bifurcates into two transitions* as the external field rotates away from the conducting planes. A first step observed in the magnetization, which results from the alignment of moments in ferromagnetic bands, moves to fields well below 1 T and leads to a large polarized moment of $1.3\mu_B$ per Ru when an external field is applied nearly along the c axis, while a second magnetization step shows a pronounced angular dependence and moves to fields beyond 45 T when it is applied nearly along the interplane axis. The enhancement of the quasiparticles effective mass and the change in the geometry of the Fermi surface at the transition, are indications of its itinerant metamagnetic character. We conclude that metamagnetism in $Sr_4Ru_3O_{10}$ is an orbital-dependent process involving both the alignment of moments or domains in ferromagnetic bands that are either itinerant or localized, and the polarization of an itinerant band that is in close proximity to a Van Hove singularity. One possible scenario is that the external field applied along the *ab* plane aligns the FM moments or domains producing a large internal field that couples to the lattice via magnetoelastic coupling. The concomitant changes in lattice constants could lead to the itinerant metamagnetic response, but as the field is rotated away from an in-plane direction, the metamagnetic transition would occur whenever the sum of the in-plane components of the internal field (which progressively tilts towards the c axis) and the external field is equal to the sum of both fields when $H \parallel ab$ plane. In any case, the complex and simultaneous involvement of several bands in the magnetic response has yet to be considered by theoretical treatments of metamagnetism.[1,2] We owe this complex physical behavior to the multiband nature of this compound. Orbital-dependent superconductivity in Sr_2RuO_4 (Ref. 14) and the proposed orbital-selective Mott transition in the $Ca_{2-x}Sr_xRuO_4$ system[15] are other examples of possible multiband behavior in the ruthenates. Band-structure calculations for $Sr_4Ru_3O_{10}$ would be highly desirable since a comparison with our experimental Fermi-surface determination could clarify the proposed existence of localized bands.[8]

ACKNOWLEDGMENTS

We acknowledge useful discussions with P. B. Littlewood and V. Dobrosavljevic. The NHMFL is supported by NSF through Grant No. NSF-DMR-0084173 and the State of Florida. Y.J.J. acknowledges support from the NHMFL-Schuller program. Z.Q.M. acknowledges the Louisiana Board of Regents fund through Grant No. LEQSF(2003-06)-RD-A-26 and the pilot fund NSF/LEQSF(2005)-pfund-23 as well as support from the NHMFL's visiting scientist program (VSP). K.S. also acknowledges the NHMFL VSP. L.B. was supported by the NHMFL in-house program.

*Present address: National Institute for Materials Science, Sengen, Tsukuba 305-0047, Japan.

[1] E. Stryjewski and N. Giordano, Adv. Phys. **26**, 487 (1977).

[2] B. Binz and M. Sigrist, Europhys. Lett. **65**, 816 (2004), and references therein.

[3] R. S. Perry, L. M. Galvin, S. A. Grigera, L. Capogna, A. J. Schofield, A. P. Mackenzie, M. Chiao, S. R. Julian, S. I. Ikeda, S. Nakatsuji, Y. Maeno, and C. Pfleiderer, Phys. Rev. Lett. **86**, 2661 (2001); S. A. Grigera, R. S. Perry, A. J. Schofield, M. Chiao, S. R. Julian, G. G. Lonzarich, S. I. Ikeda, Y. Maeno, A. J. Millis, and A. P. Mackenzie, Science **294**, 329 (2001).

[4] S. A. Grigera, P. Gegenwart, R. A. Borzi, F. Weickert, A. J. Schofield, R. S. Perry, T. Tayama, T. Sakakibara, Y. Maeno, A. G. Green, and A. P. Mackenzie, Science **306**, 1154 (2004).

[5] A. G. Green, S. A. Grigera, R. A. Borzi, A. P. Mackenzie, R. S. Perry, and B. D. Simons, Phys. Rev. Lett. **95**, 086402 (2005).

[6] G. Cao, L. Balicas, W. H. Song, Y. P. Sun, Y. Xin, V. A. Bondarenko, J. W. Brill, S. Parkin, and X. N. Lin, Phys. Rev. B **68**,

174409 (2003).
[7] M. K. Crawford, R. L. Harlow, W. Marshall, Z. Li, G. Cao, R. L. Lindstrom, Q. Huang, and J. W. Lynn, Phys. Rev. B **65**, 214412 (2002).
[8] R. Gupta, M. Kim, H. Barath, S. L. Cooper, and G. Cao, Phys. Rev. Lett. **96**, 067004 (2006).
[9] W. Bao, Z. Q. Mao, M. Zhou, J. Hooper, J. W. Lynn, R. S. Freitas, P. Schiffer, Y. Liu, H. Q. Yuan, and M. Salamon, cond-mat/0607428 (unpublished).
[10] Z. Q. Mao, M. Zhou, J. Hooper, V. Golub, and C. J. O'Connor, Phys. Rev. Lett. **96**, 077205 (2006).
[11] M. Zhou, J. Hooper, D. Fobes, Z. Q. Mao, V. Golub, and C. J. O'Connor, Mater. Res. Bull. **40**, 942 (2005).
[12] Y. Xin, G. Cao, and J. E. Crow, J. Cryst. Growth **252**, 372 (2003).
[13] R. A. Borzi, S. A. Grigera, R. S. Perry, N. Kikugawa, K. Kitagawa, Y. Maeno, and A. P. Mackenzie, Phys. Rev. Lett. **92**, 216403 (2004).
[14] D. F. Agterberg, T. M. Rice, and M. Sigrist, Phys. Rev. Lett. **78**, 3374 (1997).
[15] V. I. Anisimov, I. A. Nekrasov, D. E. Kondakov, T. M. Rice, and M. Sigrist, Eur. Phys. J. B **25**, 191 (2002); A. Koga, N. Kawakami, T. M. Rice, and M. Sigrist, Phys. Rev. Lett. **92**, 216402 (2004), and references therein.